COMPUTED AND MEASURED HEMODYNAMICS IN A COMPLIANT TAPERED FEMORAL ARTERY

Rupak K. Banerjee (1), Lloyd H. Back (2)

(1) Department of Mechanical Engineering
University of Cincinnati
Cincinnati, OH 45221-0072

(2) Jet Propulsion Laboratory
California Institute of Technology
Pasadena, CA 91109

ABSTRACT

Using measured flow parameters, vessel dimensions and blood viscosity, this study presents flow, pressure, and displacement computation and validation in a mildly tapered compliant femoral artery of a living dog. This analysis compares the results of a rigid wall and an elastic wall with experimental data. The compliant wall model is more in agreement with the experimental data, particularly during the systolic phase of the pulse cycle, than the rigid wall results.

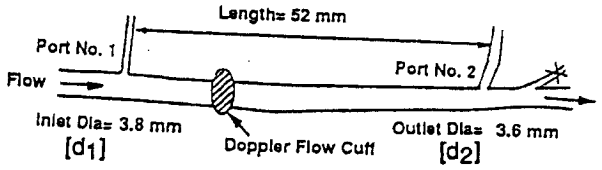

Figure 1: X-ray tracing of portion of the femoral artery of a living dog. Ligated small branch arteries are marked port No. 1 and 2.

INTRODUCTION

The arterial wall is complex, being anisotropic (elastin, collagen, smooth muscle), viscoelastic (creep, stress relaxation, hysteresis), and under a mean and fluctuating state of three-dimensional stresses, it is very difficult to specify its dynamic behavior with certainty in computational methods. Further, there are concerns about the reliability of *in vivo* measurements, and the appropriateness of the method of flow computation with regard to the non-Newtonian viscosity of blood, wall and inlet boundary conditions, and handling of the nonlinear convective acceleration terms and coupling of the pressure and velocity fields during the cardiac cycle. Thus, such a combined experimental-calculation approach is not straightforward.

Details of the finite element method (FEM) [1] for a rigid wall were given by Banerjee et al. [2, 3]. The flow simulations were carried out by solving the mass and momentum equations for pulsatile laminar blood flow using a Galarkin FEM. The Carreau model was used for shear rate dependent viscosity of blood with local shear rate calculated from the velocity gradient through the second invariant of the rate of strain tensor [4]. There is relatively unimportant elastic and time relaxation effects, which is believed to be a reasonable approximation for blood flow through arteries of the size of the femoral in a dog.

METHODS

A tracing of the X-ray of a portion of the femoral artery of a dog where the measurements were made previously at USC School of Medicine is shown in Fig. 1. The pressure drop across the segment is measured by using two small branch arteries, which are ligated and connected by tubing to a Validyne transducer. The cuff for the Doppler flow meter is located near the first branch as shown in Fig. 1. The vessel segment (Fig. 1) is simplified and kept to be relatively straight with mild taper. The vessel diameter at the first branch tap is $d_1 = 3.8$ mm, and at the second branch tap is $d_2 = 3.6$ mm. The axial distance between the branch pressure taps is 52 mm.

The mathematical modeling of compliant wall (with finite thickness) problems, which needs fluid-wall-interaction capabilities [5], requires the concurrent application of techniques from Computational Fluid Dynamics (CFD), Computational Solid Dynamics (CSD) and Computational Mesh Dynamics (CMD) fields. In the solution strategy adopted, all the three steps are performed sequentially.

The CFD step consists the solution of the flow problem on a given mesh. The exchange of information with the CSD problem happens at the fluid-wall interface. In unsteady flow problems, the velocities at the interface are computed as part of the CSD step and applied as boundary conditions for the N.S. equations. The exchange of information with the CMD step is done via the repositioning of the

nodes of the fluid domain, after each update of the configuration of the structure.

For the solution of the CFD step, fluid-wall-interaction problems are typically moving boundary problems with prescribed (or zero) boundary conditions at the interface. Moving boundary problems are addressed with the Arbitrary Lagrangian Eulerian (ALE) formulation. In unsteady simulations, the advection term is modified via the so-called mesh velocity. Accordingly, for an incompressible flow, the ALE Navier Stokes equations are:

$$\left.\begin{aligned} \rho\frac{\partial u_i}{\partial t} + \rho u_{i,j}(u_j - u_i) &= \sigma_{ij,j} + \rho f_i \\ u_{j,j} &= 0 \end{aligned}\right\} \qquad (1, 2)$$

The loads needed for coupling with the structural problem are computed with a consistent residual formulation. They have exactly the same discretization error.

The CSD step solves the momentum equations (cast in terms of displacements) in the parts of the domain that are declared as deformable arterial wall. The CSD step exchanges information with the CFD and CMD step at the fluid-wall interface nodes. Loads are received from the CFD step and velocity boundary conditions are returned to the N.S. Equations. The displacements, solution of the CSD problem, are used as boundary conditions for an elastostatic type problem, which adjusts the nodes in the interior of the domain. The structural domain of the fluid-wall-interaction problem is described by the elastostatic equations:

$$\rho\ddot{d}_i = \sigma_{ij,j} + \rho\bar{f}_i \qquad (3)$$

$$\sigma_{ij}n_j = \overset{S}{t}_i \qquad (4)$$

At each time t, equations 3 and 4 represent the balance between inertia forces, stress tensor and applied forces inside the body and the balance between the stress tensor and the applied stress on the external boundaries, respectively.

The equilibrium conditions must be complemented by the constitutive equation, which links stress and strain.

$$\sigma_{ij} = D_{ijkl}\varepsilon_{kl} \qquad (5)$$

The equilibrium equations are usually solved via a Lagrangian formulation. The Total Lagrangian (TL) formulation uses the initial configuration as reference configuration, while the Updated Lagrangian (UL) uses the most recent configuration. Both formulations involve the use of appropriate stress and strain measures. For the case of large deformations but small strains the constitutive equations are very similar to the ones used for small deformations.

RESULTS AND DISCUSSION

Computations were carried out consistent with the calibrated Doppler flow meter. The flow signal was tri-phasic with a brief period of reverse flow during the early part of diastole [3]. Using a digital voltmeter, the time-averaged blood flow velocity, u_a = 15.1 cm/sec, and the time averaged pressure drop Δp_a = -0.59 mmHg were obtained. The resting heart rate was 128 beats/min, the period T of a heartbeat was 0.47 sec. Measurement of the viscosity of the dog's blood at *in-vivo* temperature gives η =0.037 poise, and the measured blood density, ρ, was 1.04 gm/cm^3. Details of computational results for a rigid wall were given by Banerjee et al. [3] and thus are not repeated here.

Figure 2 shows the comparison of temporal variation of pressure drop between port No. 1 and port No. 2 for experimental measurements along with the rigid and the compliant wall computational models. In general, the trend and the magnitude of pressure drop between experimental & compliant wall computations during systole and diastole showed better agreement as compared to near rigid wall computation. At peak systole, the pressure drop for compliant wall was within 15% of the experimental measurement whereas a similar comparison during peak diastole was within 34%. More importantly, the phase difference during systole for both experimental and the compliant wall computation model showed excellent agreement as compared to the rigid wall computation model. However during diastole, the phase difference for both the rigid and the compliant wall computations remain out of phase when compared with experimental data. Thus, the compliant wall model is more in agreement with the experimental data, particularly during the systolic phase of the pulse cycle, than the rigid wall results.

Arterial wall movement shows that the radial displacement of the wall follows the velocity and pressure pulse. Peak radial displacement is calculated to be 0.0047 cm whereas the average radial displacement is about 0.0037 cm. Compliant wall model shows that at port 1 there is about 0.5% displacement during the peak systole.

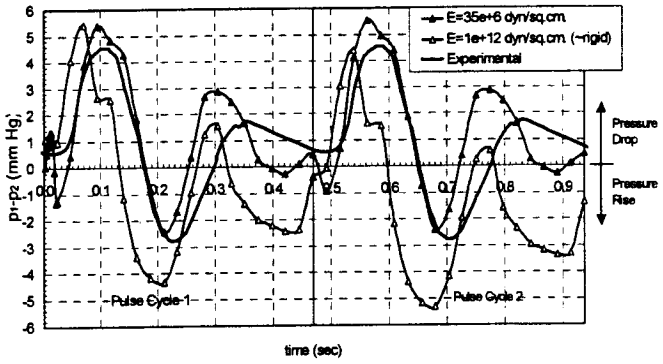

Figure 2: Comparison of temporal variation of pressure drop between port No. 1 and port No. 2 for experimental measurement with the rigid and the compliant wall computation models.

REFERENCES

1. Baker, A.J., 1983, *Finite Element Computational Fluid Mechanics*, Hemisphere Publ. Co., Chap. 4, pp. 153-230
2. Banerjee, R.K., Back, L.H., Back, M.R., and Cho, Y.L., 1999, "Catheter Obstruction Effect on Pulsatile Flow Rate – Pressure Drop During Coronary Angioplasty" ASME J. of Biomech. Engrg, Vol. 121, pp. 281-289.
3. Banerjee, R. K., Back, L.H., and Cho, Y. I., 2000, "Computational fluid mechanics (CFD) modeling techniques, using finite element methods, and application methods in arterial blood flow" *Biomechanics Systems Techniques and Applications: Biofluid Methods in Vascular and Pulmonary Systems*, CRC Press, Vol. 4, Chapter 8, 2000.
4. Cho, Y.I., and Kensey, K.R., 1991, "Effects of the non-Newtonian Viscosity of Blood on Flows in a Diseased Arterial Vessel: Part 1, Steady Flows," Biorheology. Vol. 28., 241-262.
5. FIDAP Manual, 2000, Fluent Incorporated, Lebanon, NH.